J Mater Sci (2009) 44:5806–5814
DOI 10.1007/s10853-009-3815-y

Hydroxyapatite pattern formation in PVA gels

Yasushi Suetsugu · Dominic Walsh · Junzo Tanaka · Stephen Mann

Received: 12 June 2009 / Accepted: 18 August 2009 / Published online: 29 August 2009

Abstract Sodium hydroxide solution was allowed to diffuse from the edge of an acidic poly(vinyl alcohol) gel sheet containing dissolved calcium and phosphate ions, and calcium phosphate was observed to precipitate as the pH rose. The precipitation pattern changed depending on the solute concentration near the reaction front; precipitate "walls" were formed in areas in which the calcium phosphate concentration was higher or the sodium hydroxide concentration was lower than the conditions for homogeneous precipitation, and within a very limited concentration combination of calcium phosphate and sodium hydroxide, a regular stripe pattern with a pitch of about 100 μm was formed. The calcium phosphate precipitate obtained was a single phase of hydroxyapatite. It was also found that apatite ceramic sheets with periodic porous structures or with undulate patterns could be manufactured by sintering gels with stripe patterns.

Introduction

When a solution of external electrolyte is allowed to diffuse into a gel containing internal electrolyte under a certain condition, a stripe pattern of periodic precipitation forms; a typical example has long been known as Liesegang ring [1, 2]. Much experimental and theoretical research has been performed on the Liesegang phenomenon and similar pattern formation caused by reaction–diffusion mechanisms [3–17].

Periodicities of generally known Liesegang patterns are in the order of millimeters. However, Hantz [18] reported that when a sodium hydroxide solution was diffused from the edge of a poly(vinyl alcohol) (PVA) gel sheet containing dissolved copper chloride, consequent copper oxide precipitation formed a fine stripe pattern of 10-μm-order periodicity. In addition, Imai et al. [19, 20] prepared hydroxyapatite (HAp) lamellar structure with micrometer-order periodicity mainly by diffusion of calcium nitrate solution into a poly(acrylic acid) gel containing ammonium phosphate.

Calcium phosphate, especially in the form of HAp, is well known as the main inorganic component of hard tissues such as bone and teeth, and is a superior biomaterial for use in implants due to its very high biocompatibility. It is also promising as a possible cell culture substrate for cell engineering.

Because affinity with biological cells is thought to be strongly influenced by the microstructure of the substrate, there have been some attempts to investigate the behavior of cells, such as osteoblasts, cultured on substrates containing microgrooves coated with HAp [21, 22]. HAp ceramics possessing 10-μm-order micropatterned surfaces are promising materials for cell engineering, but micromachining of ceramics is generally expensive. Microfabrication by a simple reaction–diffusion process may therefore be a useful tool in this field. Liesegang patterns of calcium phosphate were reported in some works [23–26], but fabrication of microstructured HAp ceramics utilizing the similar phenomenon was performed only by abovementioned Imai

Y. Suetsugu (✉)
Biomaterials Center, National Institute for Materials Science, 1-1 Namiki, Tsukuba, Ibaraki 305-0044, Japan
e-mail: SUETSUGU.Yasushi@nims.go.jp

D. Walsh · S. Mann
School of Chemistry, University of Bristol, Bristol BS8 1TS, UK

J. Tanaka
Department of Metallurgy and Ceramics Science, Tokyo Institute of Technology, 2-12-1 Ookayama, Meguro, Tokyo 152-8550, Japan

et al. [19, 20]. In the present study, utilizing a periodical precipitation in a gel sheet, we attempted to create two-dimensional regular stripe patterns of HAp with 10-μm-order pitch anticipating an application to cell culture substrates. The two-dimensional gel-based experimental system also enabled an in situ observation of reaction–diffusion process forming micropatterned precipitation.

Experimental

For successful creation of a micropattern in a thin gel sheet, the gel must have a low tendency to swell or shrink against changes in pH or electrolyte concentration. For this reason, PVA gel chemically crosslinked by glutaraldehyde is preferable to gelatin, agar, poly(acrylic acid) or poly(acrylamide) gel. However, this crosslinking reaction requires acidic conditions, which are not desirable for precipitation of HAp by diffusion of calcium salt into the gel containing dissolved phosphate ions. As the gel sheet is prepared between glass plates, deacidification of the crosslinked acidic gel and impregnation of phosphate ions is difficult. Hence, acidic PVA gel containing both phosphate and calcium ions was employed for this work; sodium hydroxide solution was allowed to diffuse into the gel to raise the pH, causing precipitation of HAp.

To prepare gels containing calcium phosphate ions, the following solutions were prepared in advance. The water used for all experiments was purified using an Elga PURELAB Ultra system.

First, 37% hydrochloric acid (Aldrich) was diluted to a concentration of 12.3 wt%. Calcium phosphate powder (Sigma) was dissolved in it to make an aqueous solution with a concentration of 2 and 1.2 M of calcium and phosphate, respectively; the solution could be described as a 0.2 M HAp solution, given that the chemical formula of HAp is $Ca_{10}(PO_4)_6(OH)_2$. The pH was about 0.1, indicating that the phosphate groups existed as H_3PO_4 and $H_2PO_4^{2-}$.

PVA (Fluka, molecular weight 72000) was added to water and vigorously stirred for 4 h at 75 °C to obtain a 8.6 wt% aqueous solution. Crosslinking was carried out by adding glutaraldehyde (Aldrich), which was diluted and prepared as a 0.1 M aqueous solution in advance.

The prepared HAp solution, the PVA solution and water were mixed at the specified ratios, followed by addition of the glutaraldehyde solution. The concentrations of PVA and glutaraldehyde were set to 4.3 wt% (1 M vinyl alcohol monomer unit) and 5 mM (0.5 mol% against the monomer units of PVA), respectively.

The mixture was placed in an ultrasonic cleaner for about 10 s to exclude air bubbles, and then 200 μL was dropped onto a microscope slide and covered with a cover glass of 22 × 50 mm to spread the mixture at a thickness of

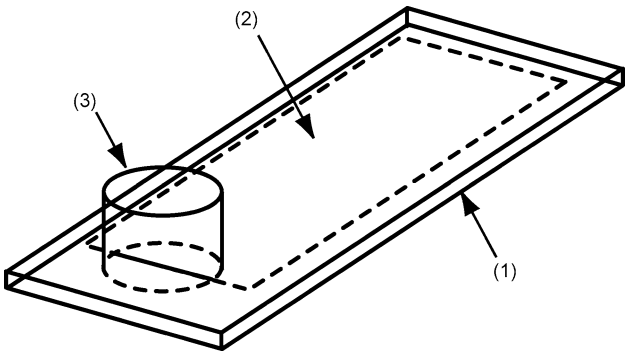

Fig. 1 Schematic illustration of gel container for patterning experiment. (1) Slide glass, (2) cover glass overlaid on PVA gel sheet, (3) plastic cylinder. *Dashed lines* indicate the area sealed by epoxy resin

100–200 μm. Gelation began in about 10 min and was completed after about 1 h. After gelation had taken place, the circumference of cover glass was sealed with epoxy adhesive to prevent drying. Part of one shorter edge was not sealed, and a short plastic cylinder was attached to the unsealed part as a sodium hydroxide reservoir (Fig. 1). An aqueous solution (200 μL) of sodium hydroxide (Fluka), prepared to the specified concentrations, was placed in the plastic cylinder, after which the cylinder was covered tightly with a lid, and the samples were kept still at room temperature until diffusion was complete. The precipitation patterns that formed in the gel sheet following diffusion of sodium hydroxide were observed using an optical microscope. After diffusion, the samples were washed by soaking in water, followed by drying and/or calcination, and then coated with platinum/palladium or carbon for observation and analysis using a scanning electron microscope (SEM, JEOL JSM-6330F) equipped with an Energy-Dispersive X-ray Analyzer (EDXA, Oxford Instruments ISIS300). Parts of the calcined samples were roughly ground and dispersed into ethanol, and samples for transmission electron microscopy (TEM, JEOL JEM-2010) were prepared by air-drying droplets of the suspension on carbon-coated copper grids.

Laser Raman microscopy analysis was performed using a Renishaw RM system with an Ar ion laser (wavelength 514 nm), observing precipitation during diffusion. To avoid scattering from glass, the gel sample for Raman microscopy was prepared with a thickness of 1 mm. For powder X-ray diffraction (XRD) and Fourier transform infrared spectroscopy (FTIR), a similar gel (2 mL) was prepared in a glass tube with a diameter of 2 cm, onto which an equal amount of sodium hydroxide solution was poured from the top. The XRD experiment was performed using a Bruker D8 Advance system with CuKα radiation (40 kV, 40 mA). The FTIR spectra were measured using a Perkin-Elmer Spectrum One system with KBr disks containing about 1 wt% of sample. Background data were measured with air.

Results

Change in precipitation pattern during diffusion

The precipitation pattern changed as sodium hydroxide diffusion proceeded. Typical precipitation behavior is described below for a sample with a HAp concentration of 70 mM (calcium ion concentration of 0.70 M and phosphate group concentration of 0.42 M) and a sodium hydroxide solution concentration of 2 M.

Figure 2 shows the gel sheet after diffusion has proceeded to the far end of the sheet. When the sodium hydroxide solution first touches the edge of the gel, a "wall" of precipitate is formed at the interface between the gel and the sodium hydroxide solution. Diffusion begins from one part of the wall and spreads in a fan-like shape to an area without precipitation. The boundary between regions where precipitation has already occurred and regions without precipitation is very sharp; this boundary is henceforth referred to as the reaction front. The speed of progression of the reaction front falls gradually, until one part suddenly halts to form a new wall, which extends along the reaction front (Fig. 3). When the whole reaction front becomes a wall, diffusion halts again. The discrete sequence of walls forms by repetition of this process. This wall may be considered to be similar to the "passive edge" or "passive border" in the works of Hantz et al. [18, 27]. While most of the walls are 10–100 μm thick, there are also some up to 0.5 mm thick, and some show a lamellar structure (Fig. 4). The maximum speed of advance of the reaction front, observed immediately after it had arisen from part of a previous wall, was 4 μm/s (with a sodium hydroxide concentration of 8 M). When the speed of progress is more than 1 μm/s, crystals with hexagonal or hexagonal star-like plate shapes are observed to grow behind the reaction fronts (Figs. 3 and 4).

As diffusion continues, the space between walls widens gradually and the direction of the walls becomes parallel to

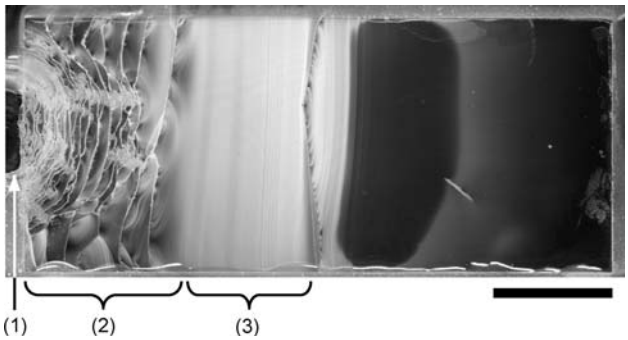

Fig. 2 Precipitation pattern on PVA gel sheet with HAp concentration of 70 mM and NaOH concentration of 2 M. NaOH diffused from left to right. (1) NaOH reservoir, (2) walls, (3) stripe pattern. Taken by a scanner with reflection light. Scale bar = 10 mm

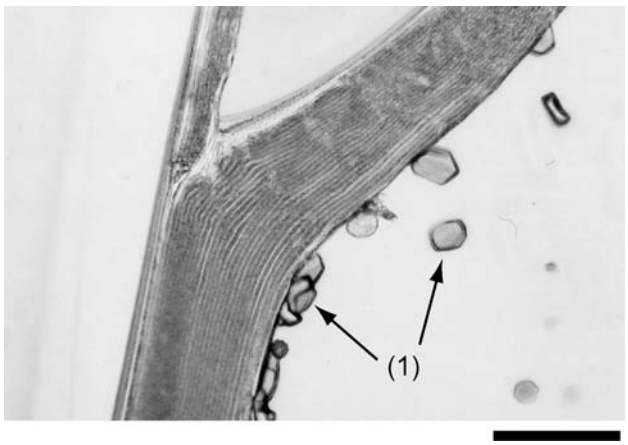

Fig. 4 Wall with lamellar structure. NaOH diffused from left to right. (1) Hexagonal crystals. Taken with transmission light. Scale bar = 200 μm

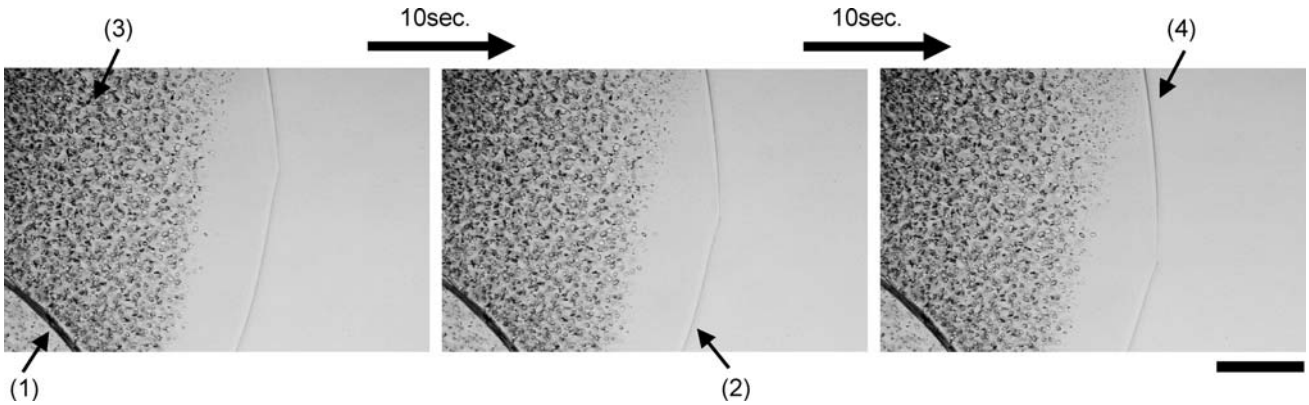

Fig. 3 Progression of reaction front generating a new wall. Photos were taken at 10-s intervals with transmission light. (1) Previous wall, (2) reaction front, (3) hexagonal crystals, (4) new wall. Scale bar = 200 μm

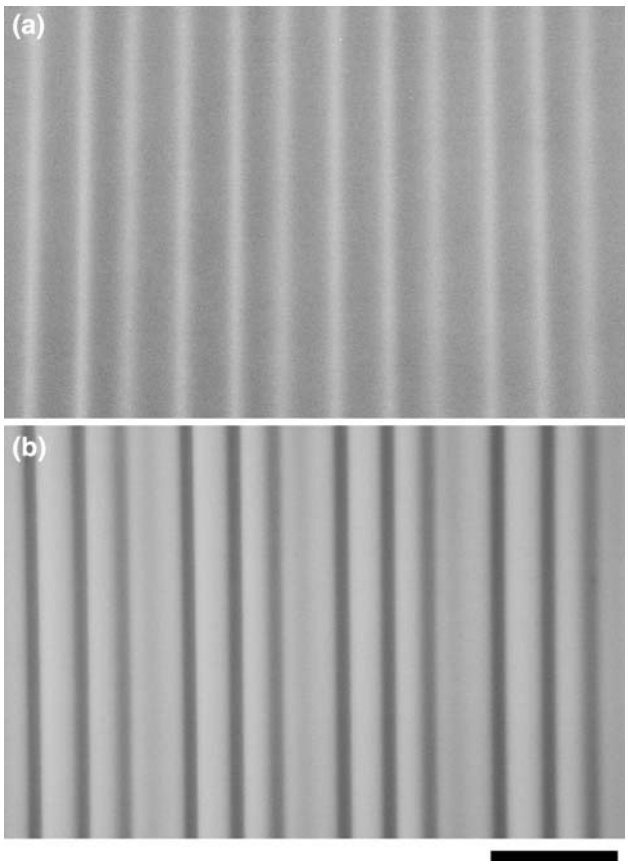

Fig. 5 Stripe patterns of precipitate in gel. **a** Taken with reflection light. **b** With periodicity of density; taken with transmission light. Scale bar = 200 μm

the interface between the gel and the sodium hydroxide solution. Nothing interesting occurs for a while after this point, but then, when the speed of reaction front becomes less than 0.1 μm/s without formation of a new wall, precipitation begins to form in a striped pattern with intervals of 50–200 μm (Fig. 5). As diffusion progresses further, this stripe pattern increases in sharpness and its spacing becomes more regular. Some of the stripe patterns show periodicity in terms of thickness (Fig. 5b). Some time later, progress of the diffusion front halts again to form another wall, and in some cases this is followed by reestablishment of stripe-patterned precipitation. Eventually, because of the gradual decrease in the density of precipitation, precipitation can no longer be observed.

Crystals constituting the precipitate

Figure 6 shows SEM images taken from a viewpoint almost perpendicular to the face of the gel sheet. Figure 6a shows parts of the fan-like stripe pattern, and a wall. Due to the drying process, the part of the sample with a high precipitation density has a protuberant appearance. Figure 6b shows nanocrystals of the main component of the precipitation. Each crystal has a rice-grain-like shape with a length of 100–200 nm; these are common to walls, homogeneous precipitation areas and stripe patterns. Calcium, phosphorus and oxygen were detected in these grains by EDXA. Figure 6c shows part of a wall with a lamellar structure. While the area that was attached to the glass has a smooth surface, the inside is composed of rice-like grains similar to those seen in Fig. 6b. Figure 6d shows hexagonal plate crystals grown in the area ahead of a wall. The whole structure is covered with rice-like crystals. While substantial crystal plates may be observed in a sample that was dried within 24 h after crystal growth, as shown in Fig. 6e, mature samples that were dried after a sufficiently long period show only hollow structures (Fig. 6f). Only calcium and oxygen were detected in these crystals by EDXA.

A TEM image and the electron diffraction pattern of one of the rice-like grains are shown in Fig. 7. The pitch of the fringe (0.82 nm) corresponds with the *d*-value of the lattice plane (100) of HAp, and its direction conforms to the major axis of the particle. The electron diffraction image of the same field coincides with the a^*-c^* reciprocal lattice plane of the HAp structure, with the c^*-axis conforming to the major axis of the particle. The *d*-value of (100) and the dimensions of reciprocal lattice of HAp used here were calculated from the data reported by Hughes et al. [28].

Micro-Raman spectra measured in some parts of the gel during diffusion are shown in Fig. 8. The speed of the reaction front during measurement was about 0.1 μm/s. At the reaction front (c), the precipitate was mainly composed of brushite ($CaHPO_4{\cdot}2H_2O$), which changed gradually to HAp (d, e); after about 1 h, only HAp was detected (f). Furthermore, after several days (g), ripening of the HAp crystals took place. The peak at 890 cm^{-1}, attributed to H_3PO_4 dissolved in the original gel (a), decreased in the region ahead of the reaction front (b), indicating that phosphate groups migrated to the reaction front as precipitation continued. The hexagonal crystals that grew between the reaction front and the wall were confirmed to be calcium hydroxide (h), which disappeared with time.

XRD patterns of the precipitates are shown in Fig. 9. Figure 9a shows a sample, including gel, which was dried and pulverized within 24 h after precipitation. Figure 9b shows an older sample of the precipitate, also after drying; Fig. 9c shows the same sample after water rinsing followed by calcination at 800 °C. Figure 9a demonstrates that calcium hydroxide, sodium chloride and sodium carbonate monohydrate are present in addition to HAp. The presence of carbonate ions in the system is mainly due to the dissolution of carbon dioxide from the air in the sodium hydroxide solution. The amount of brushite present was below the detection limit of the XRD method. The diffraction peaks shown in Fig. 9b are almost the same as those of Fig. 9a except that the calcium hydroxide peaks

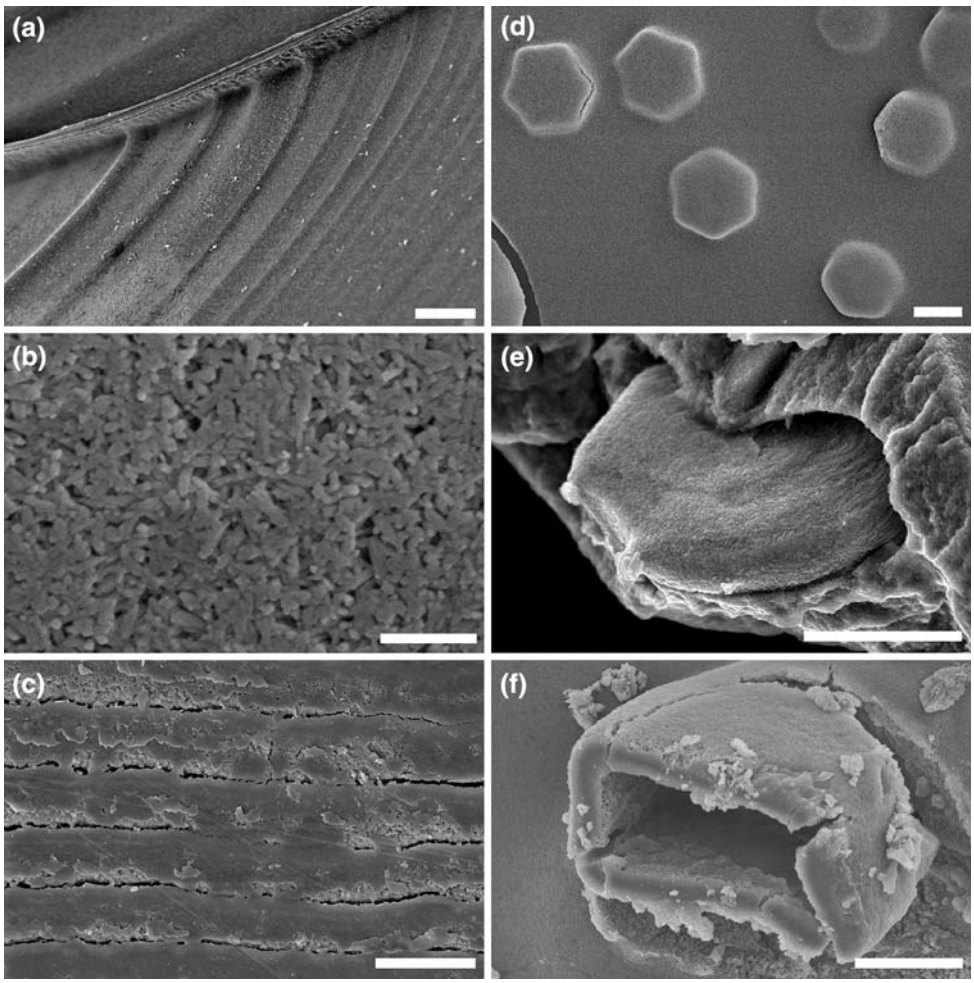

Fig. 6 SEM images of precipitate. **a** Wall and fan-like stripe pattern, rinsed with water and dried. **b** Precipitate nanocrystals, calcined at 600 °C after water rinsing. **c** Wall with lamellar structure, calcined at 600 °C after water rinsing. **d** Hexagonal plates, calcined at 600 °C after water rinsing. **e** Hexagonal plates immediately after growth, dried. **f** Hexagonal plate over 24 h after growth, dried. Scale bars represent 100 μm (**a**, **c**), 500 nm (**b**), 10 μm (**d**–**f**)

have disappeared. After water rinsing and calcination (Fig. 9c), only HAp was detected.

Figure 10 shows FTIR spectra of the samples. Figure 10a and c represent the samples whose XRD patterns are shown in Fig. 9a and b, respectively. Figure 10b shows the same sample after water rinsing but before calcination. Figure 10a shows HAp with low crystallinity and carbonate ions in the form of sodium salt. After water rinsing (Fig. 10b), which removes the sodium salt, residual carbonate ions, detected as a small peak at around 1500 cm^{-1}, are present in the phosphate site (B-site) of HAp structure. After calcination (Fig. 10c), only the HAp single phase with a small amount of carbonate ions is detected.

HAp ceramic sheet with stripe pattern

A gel sheet with stripe-pattern precipitation with a periodicity of 90 μm was sintered at 1200 °C for 1 h and observed by SEM. Before sintering, part of the gel sheet was fixed on HAp ceramic substrate with PVA aqueous solution as an adhesive, and the other part was set loose and allowed to shrink freely. SEM images of the resulting sample are shown in Fig. 11. The sample fixed on the substrate (Fig. 11a, b) showed a stripe pattern consisting of variations in porosity. The periodicity of the stripe pattern was maintained at 90 μm, and the size of the grains was about 1 μm. When the sample was allowed to shrink freely during heating, it became a ceramic sheet with an undulate pattern with a pitch of about 50 μm (Fig. 7c, d). Grain growth was more marked than in the fixed samples; particles of up to 10 μm in diameter were observed. The thin part of the sintered samples was of less than 10 μm thick and macroscopically transparent. This property was advantageous considering the application for cell culture substrates because it could enable an optical observation of cells cultured on them.

Change in precipitation pattern with different salt concentrations

A change in the precipitation pattern near the interface of the gel and sodium hydroxide solutions was observed when

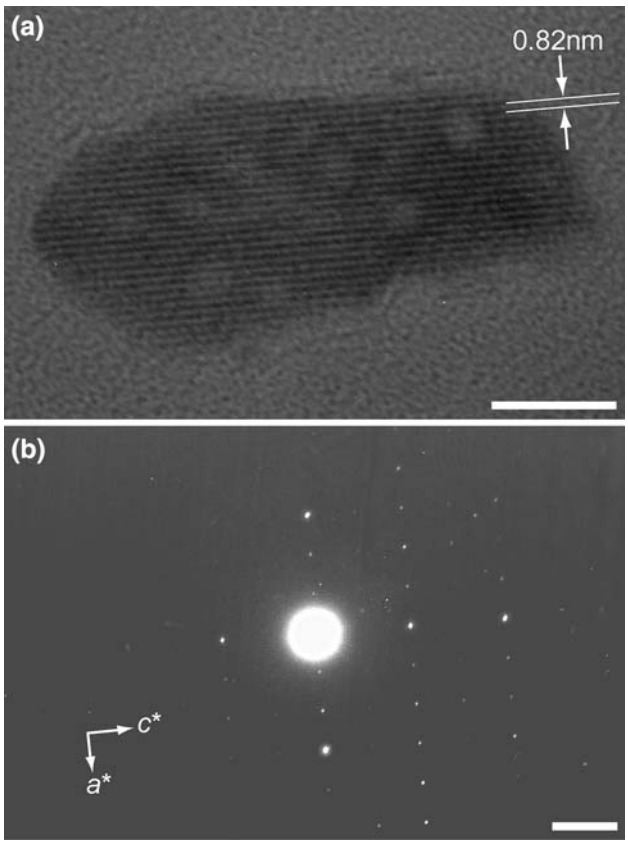

Fig. 7 TEM image (**a**) and electron diffraction pattern (**b**) of nanocrystals. Scale bars represent 10 nm (**a**), 2 nm^{-1} (**b**)

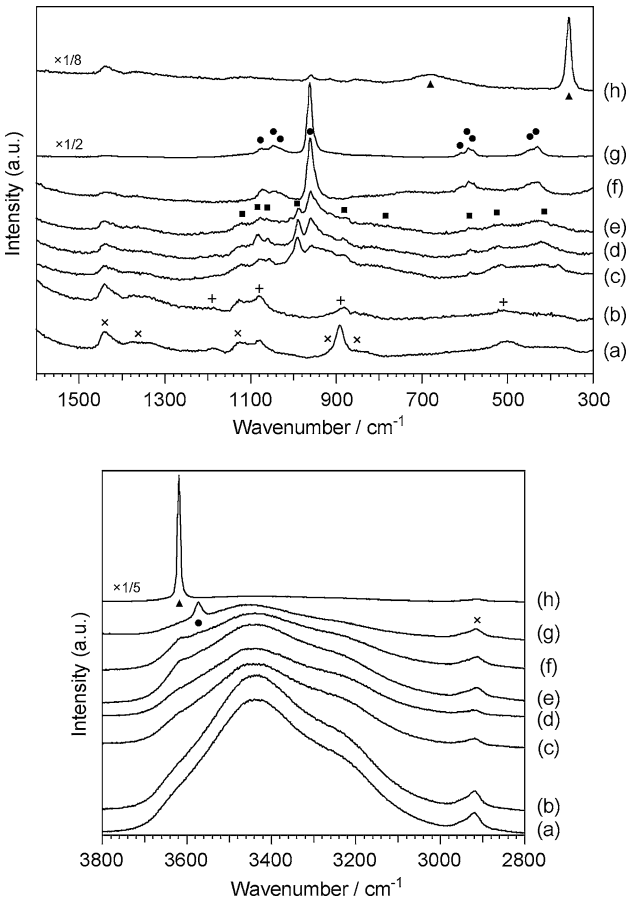

Fig. 8 Raman spectra of various parts of the gel during diffusion of sodium hydroxide: (*a*) before sodium hydroxide diffusion, (*b*) 400–500 μm ahead of the reaction front, (*c*) 0–100 μm behind the reaction front, (*d*) 100–200 μm behind the reaction front, (*e*) 200–300 μm behind the reaction front, (*f*) 300–400 μm behind the reaction front, (*g*) precipitate after aging (10 days after precipitation), (*h*) hexagonal plate-form crystal (immediately after crystal growth). Attribution of main peaks: (▲) $Ca(OH)_2$ [29]; (●) HAp [26, 30]; (■) brushite [31]; (+) phosphate ions in solution phase; (×) PVA [32]. Other peaks: 3700–3000 cm^{-1}, H_2O; 3619 cm^{-1}, OH^- in solution

the concentrations of calcium phosphate in the gel and sodium hydroxide were changed; this is shown in Fig. 12. When the calcium phosphate solution was dilute and the concentration of sodium hydroxide was high, a wall did not form. Crystals of calcium hydroxide grew ahead of the walls only when the substrate was rich in both calcium phosphate and sodium hydroxide. Stripe patterns formed under limited circumstances when the concentration of HAp was about 10 mM and that of sodium hydroxide was 0.5–1 M.

Discussion

In this section, based on the results obtained in this study, we consider from a qualitative point of view the diffusion of sodium hydroxide solution in gel containing calcium phosphate and the generation of precipitation patterns.

First, when a sodium hydroxide solution is allowed to contact with a gel which contains calcium phosphate, precipitation occurs at the reaction front, resulting in a plunge in concentration of the relevant ions in the areas adjacent to the reaction front. At the area corresponding to A, B or C in Fig. 12, due to high precipitation speed, a wall forms. Progression of the reaction front can stop completely here if the concentration of sodium hydroxide is low enough (C). With higher concentration, subsequent diffusion of sodium hydroxide from certain points on the wall can resume but results in the creation of a new lamellar wall if the calcium phosphate concentration is high enough. However, phosphate and calcium ions are supplied from ahead of the wall, gradually making the wall thicker and causing a decrease in the concentration of calcium phosphate in this region. If sodium hydroxide passes through the wall ahead of the area in which the concentration of calcium phosphate has become low, then diffusion progresses, and homogeneous precipitation spreads (D).

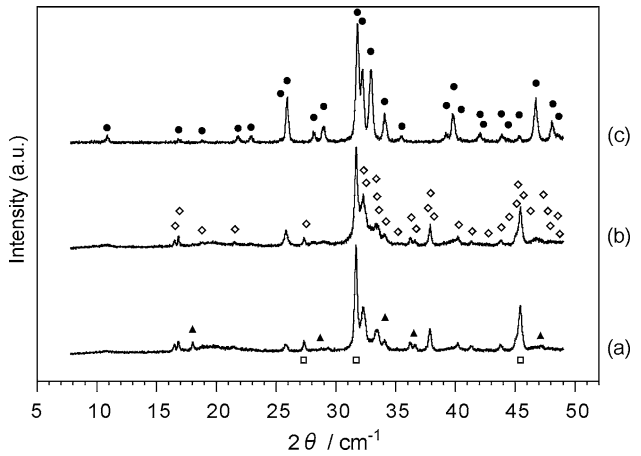

Fig. 9 Powder X-ray diffraction patterns of precipitate: (*a*) dried and pulverized within 24 h of precipitation, (*b*) dried and pulverized more than 24 h after precipitation, (*c*) sample (*b*) calcined at 800 °C after water rinsing. Peak attribution: (●) HAp (JCPDS 9-432); (◇) $Na_2CO_3{\cdot}H_2O$ (JCPDS 8-448); (▲) $Ca(OH)_2$ (JCPDS 44-1481); (□) NaCl (JCPDS 5-628)

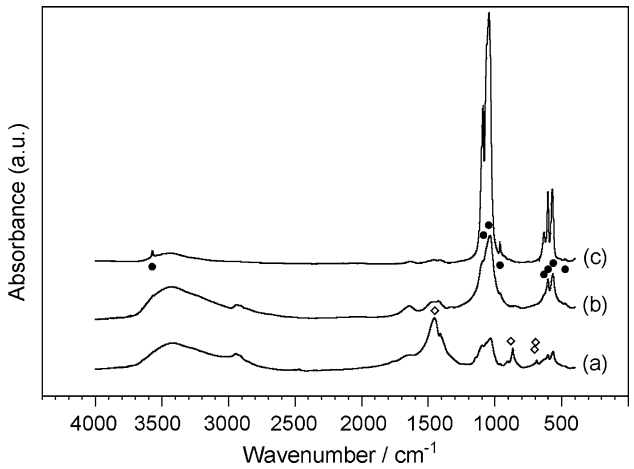

Fig. 10 FT-IR spectra: (*a*) sample dried and pulverized within 24 h after precipitation, (*b*) sample (*a*) after water rinsing and drying, (*c*) sample (*b*) calcined at 800 °C. Attribution of main peaks: (●) HAp [26, 30]; (◇) $Na_2CO_3{\cdot}H_2O$ [33]. Other peaks: 3651 cm^{-1}, $Ca(OH)_2$ [29]; 3700–3000 cm^{-1} and 1630 cm^{-1}, H_2O; 2940 cm^{-1}, PVA; 1141 cm^{-1}, brushite [31]

In this study, because the original molar ratio of calcium and phosphate, Ca/P, in the gel is the same as that of HAp (1.67), and brushite (Ca/P = 1) precipitates first, the excess calcium ions are left unconsumed near the reaction front. If the concentrations of sodium hydroxide and residual calcium are both sufficiently high (A), crystals of calcium hydroxide grow. Some time later, as the pH rises up to neutral, brushite is converted to the HAp phase [34] via the incongruent dissolution with a hydrolysis reaction

$$10CaHPO_4 \cdot 2H_2O \rightarrow Ca_{10}(PO_4)_6(OH)_2 + 4H_3PO_4 + 18H_2O,$$

then the calcium hydroxide crystals dissolve, leaving hollows.

Meanwhile in area D, the concentration of calcium phosphate ahead of the reaction front rises, and when the combination of the concentrations of relevant ions reaches area B, a wall forms again. Thus a discrete sequence of walls is formed. However, since the calcium phosphate concentration decreases as a whole, the concentration of each ion at the point of the wall at which diffusion restarts is not always the same. Therefore, the route in which the combination of concentrations near the reaction front follows in Fig. 12 also changes. When the composition near the reaction front passes area E, a stripe pattern is formed. For example, Fig. 13 shows a sample obtained under the same conditions as that shown in Fig. 2, except that another reservoir, containing HAp solution at the same concentration as the gel, was attached at the opposite end of the gel sheet from the first reservoir, continuously supplying calcium phosphate to the gel. In contrast to the sample shown in Fig. 2, the sequence of wall formation and homogeneous precipitation repeated without formation of a wide area of fine stripes, until progression of reaction front finally stopped.

The mechanism of stripe-pattern formation resembles that of wall formation, but in this case the reaction front does not halt. Instead, in the area corresponding to area E in Fig. 12, the speed of the reaction front decreases a little when precipitation occurs, resulting in formation of the thick part of the stripe. Meanwhile, in the area ahead of the reaction front, the calcium and phosphate concentrations decrease. When the reaction front arrives in this area, the diffusion speed rises again. The process is repeated when the reaction front arrives at another area with a high calcium phosphate concentration, and thus a stripe pattern is formed.

Summary

Precipitation of calcium phosphate taking place when sodium hydroxide solution was allowed to diffuse into an acidic PVA gel sheet containing dissolved calcium phosphate was observed. The density of precipitation varied according to the change in the concentration of each ion near the reaction front eventually resulting in the formation of regular stripe patterns of HAp with 10-μm-order pitch. HAp ceramics possessing micropatterned surface prepared by sintering the gels thus obtained may be applicable as cell culture substrates.

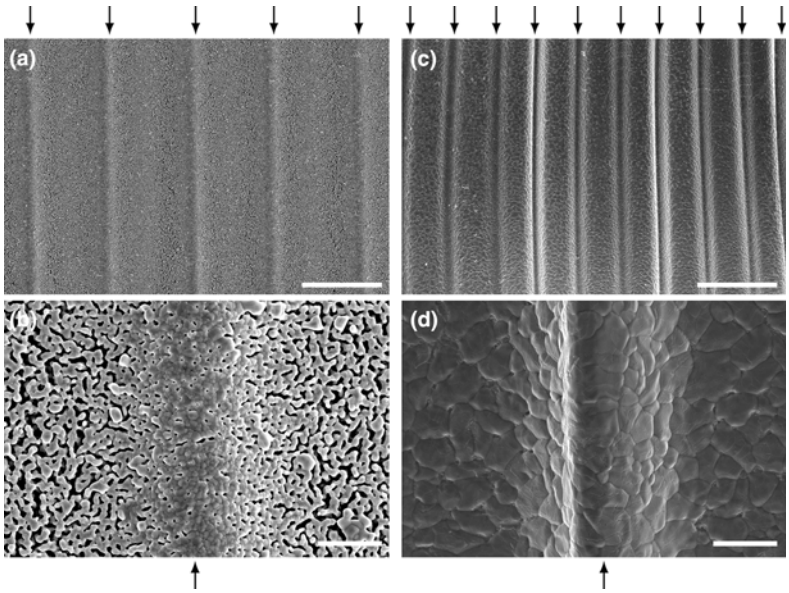

Fig. 11 HAp sintered body with stripe pattern. The *arrows* show areas with high precipitation densities before sintering: **a**, **b** area fixed on HAp substrate, **c**, **d** unattached area. Scale bars represent 100 μm (**a**, **c**), 10 μm (**b**, **d**)

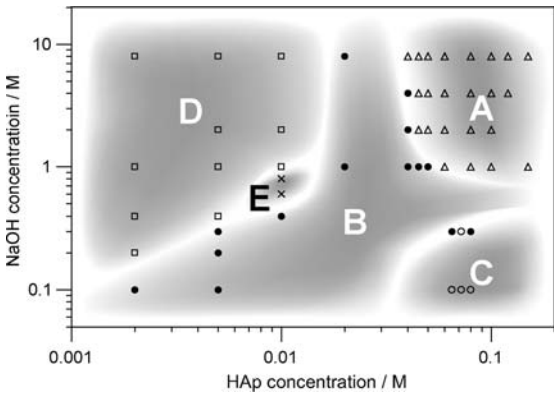

Fig. 12 Precipitation behavior near the interface with change in concentrations of calcium phosphate and sodium hydroxide. Calcium phosphate concentration is described as HAp concentration. A (△): after formation of wall, crystal growth of calcium hydroxide occurs in area ahead of wall. B (●): wall forms. C (○): wall forms and diffusion almost stops. D (□): diffusion progresses, resulting in homogeneous precipitation. E (×): diffusion progresses, resulting in stripe pattern formation

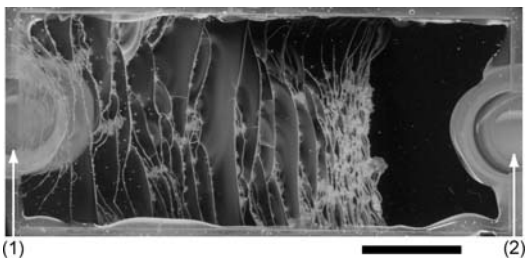

Fig. 13 Precipitation pattern in PVA gel sheet with NaOH and HAp reservoirs attached. HAp concentration: 70 mM; NaOH concentration: 2 M. NaOH diffused from left to right. (1) NaOH reservoir, (2) HAp reservoir. Taken by a scanner with reflection light. Scale bar = 10 mm

Acknowledgements The authors are very grateful to Dr. Kensuke Aoki and Dr. Alexander Kulak for helpful discussions and operation of the electron microscopes. We thank Dr. Paul May and Dr. Jacob Filik for their kind support in measurement of Raman spectra.

References

1. Liesegang RE (1896) Naturwiss Wochenschr 11:353
2. Stern KH (1954) Chem Rev 54:79
3. Henisch HK (1986) J Cryst Growth 76:279
4. Chopard B, Luthi P, Droz M (1994) Phys Rev Lett 72:1384
5. Antal T, Droz M, Magnin J, Rácz Z, Zrinyi M (1998) J Chem Phys 109:9479
6. Rácz Z (1999) Phys A 274:50
7. Droz M (2000) J Stat Phys 101:509
8. George J, Varghese G (2002) Chem Phys Lett 362:8
9. George J, Varghese G (2002) Colloid Polym Sci 280:1131
10. George J, Varghese G (2004) J Mater Sci 39:311. doi:10.1023/B:JMSC.0000007763.81805.a2
11. Grzybowski BA, Bishop KJM, Campbell CJ, Fialkowski M, Smoukov SK (2005) Soft Matter 1:114
12. Izsák F, Lagzi I (2005) J Chem Phys 122:1847071-7
13. Narita T, Tokita M (2006) Langmuir 22:349
14. Wang Y, Chan CM, Li L, Ng KM (2006) Langmuir 22:7384
15. Volfort A, Izsák F, Ripszám M, Lagzi I (2007) Langmuir 23:961
16. Jahnke L, Kantelhardt JW (2008) Eur Phys J 161:121
17. Molnár F, Izsák F, Lagzi I (2008) Phys Chem Chem Phys 10:2368
18. Hantz P (2002) Phys Chem Chem Phys 4:1262
19. Imai H, Tatara S, Furuichi K, Oaki Y (2003) Chem Commun 15:1952
20. Furuichi K, Oaki Y, Ichimiya H, Komotori J, Imai H (2006) Sci Technol Adv Mater 7:219
21. Perizzolo D, Lacefield WD, Brunette DM (2001) J Biomed Mater Res 56:494
22. Lu X, Leng Y (2003) J Biomed Mater Res A 66:677
23. Cartwright JHE, García-Ruiz JM, Villacampa AI (1999) Comput Phys Commun 121:411
24. Göbel C, Simon P, Buder J, Tlatlik H, Kniep R (2004) J Mater Chem 14:2225

25. George J, Varghese G (2005) J Mater Sci 40:5557. doi:10.1007/s10853-005-4550-7
26. Rosseeva EV, Buder J, Simon P, Schwarz U, Frank-Kamenetskaya OV, Kniep R (2008) Chem Mater 20:6003
27. Hantz P, Partridge J, Lang G, Horvat S, Ujvari M (2004) J Phys Chem B 108:18135
28. Hughes JM, Cameron M, Crowley KD (1989) Am Miner 74:870
29. Lutz HD, Möller H, Schmidt M (1994) J Mol Struct 328:121
30. Koutsopoulos S (2002) J Biomed Mater Res 62:600
31. Xu JW, Butler IS, Gilson DFR (1999) Spectrochim Acta A 55:2801
32. Thomas PS, Stuart BH (1997) Spectrochim Acta A 53:2275
33. Harris MJ, Salje EKH (1992) J Phys Condens Matter 4:4399
34. Fulmer MT, Brown PW (1998) J Mater Sci Mater Med 9:197